A&A 386, 114–123 (2002)
DOI: 10.1051/0004-6361:20020214

Astronomy & Astrophysics

Hα surface photometry of galaxies in the Virgo cluster I. Observations with the San Pedro Martir 2.1 m telescope⋆,⋆⋆

G. Gavazzi[1], A. Boselli[2], P. Pedotti[1], A. Gallazzi[1], and L. Carrasco[3,4]

[1] Università degli Studi di Milano-Bicocca, Piazza delle scienze 3, 20126 Milano, Italy
[2] Laboratoire d'Astronomie Spatiale, Traverse du Siphon, 13376 Marseille Cedex 12, France
e-mail: Alessandro.Boselli@astrsp-mrs.fr
[3] Instituto Nacional de Astrofísica, Optica y Electrónica, Apartado Postal 51. C.P. 72000 Puebla, Pue., México
e-mail: carrasco@transun.inaoep.mx
[4] Observatorio Astronómico Nacional, UNAM, Apartado Postal 877, C.P. 22860, Ensenada B.C., México

Received 3 December 2001 / Accepted 5 February 2002

Abstract. Hα imaging observations of 125 galaxies obtained with the 2.1 m telescope of the San Pedro Martir Observatory (SPM) (Baja California, Mexico) are presented. The observed galaxies are mostly Virgo cluster members (77), with 36 objects in the Coma/A1367 supercluster and 12 in the clusters A2197 and A2199 taken as fillers. Hα+[NII] fluxes and equivalent widths, as well as images of the detected targets are presented.

Key words. galaxies: photometry – galaxies: clusters: individual: Virgo

1. Introduction

One of the crucial, yet unsettled issues related to the evolution of galaxies is a robust observational determination of the present stage of star formation activity of local galaxies. By far the best tracer of the massive ($>5\ M_\odot$) star formation rate (*SFR*) in galaxies is provided by the intensity of their hydrogen recombination lines, among which primarily Hα (Kennicutt 1998). Besides having shown that the activity of star formation (per unit mass) increases along the Hubble sequence (Roberts & Haynes 1994; Kennicutt 1998), the phenomenology of the star formation properties of disk galaxies remains mostly unexplored. One of the unsettled issues refers to the environmental dependence of the mean *SFR* of galaxies. The very existence of the Schmidt law (Schmidt 1959) $\Sigma_{SFR} = A\Sigma^{\rm N}_{\rm gas}$ (Kennicutt 1998) implies that galaxies suffering from significant gas depletion, such as observed in clusters of galaxies (Giovanelli & Haynes 1985), should have their *SFR* consiredably quenched. This prediction is however controversial. If on the one hand Kennicutt (1983) found that spirals in the Virgo cluster show mean *SFR* as much as a factor of two lower than isolated galaxies, Gavazzi et al. (1998) did not confirm this evidence in the Coma and A1367 clusters. The result of Kennicutt (1983) was based on only two dozen galaxies with Hα measurements from aperture photometry, thus requiring a confirmation on a larger sample with modern imaging data.

With the aim of solving this riddle we undertook an Hα imaging survey of two optically complete samples of galaxies. The first is composed of nearly isolated objects selected from the CGCG (Zwicky et al. 1961–68) in the bridge between Coma and A1367 which we observed down to the limit of 15.7 mag. This constitutes our reference sample of non-cluster objects. The cluster sample is focused on the Virgo cluster. We concentrated the observations on cluster members ($V < 3000$ km s^{-1}) selected from the VCC catalogue of Binggeli et al. (1985) with $m_{\rm pg} < 16.0$ and with Hubble type later than S0a. The presentation of the first set of 77 Hα observations obtained with the 2.1 m telescope of the San Pedro Martir Observatory is addressed in the present paper, it continues with 95 observations carried out with the 1.2 m telescopes of the Observatoire de Haute Provence and of the Calar Alto Observatory (Boselli & Gavazzi 2002; Paper II) and with a set of observations, primarily of BCD galaxies, obtained with the INT telescope (Boselli et al. 2002; Paper III). These new observations, combined with the ones available from the literature (Kennicutt & Kent 1983; Romanishin 1990; Young et al. 1996; Koopmann et al. 2001) bring to 235 the number of Virgo galaxies with

Send offprint requests to: G. Gavazzi,
e-mail: giuseppe.gavazzi@mib.infn.it

⋆ The observatory of San Pedro Martir (Mexico) belongs to the Observatorio Astronómico Nacional, UNAM.

⋆⋆ Figure 4 is only available in electronic form at http://www.edpsciences.org

Hα data. They form a sample representative of the Hα properties of Virgo galaxies, 75% complete at $m_{\rm pg} < 16.0$ which will be analyzed in a forthcoming paper (Gavazzi et al. 2002a, in preparation, Paper IV).

2. The sample

Galaxies observed in this work have been selected from the Virgo Cluster Catalogue (VCC) of Binggeli et al. (1985), which is complete to the optical magnitude $m_{\rm pg} = 18.0$. The targets were selected using the following criteria:
$m_{\rm pg} < 16.0$.
Hubble type later than S0a (as given in the VCC).
Classified as cluster members, possible members or belonging to the W, W', M clouds or to the southern extension (Binggeli et al. 1985, 1993) matching $V < 3000$ km s^{-1}.
Because of the particular set of interferometric filters available at SPM the velocity interval of galaxies selected in this paper was narrowed to $350 < V < 3000$ km s^{-1}. In this paper we present the first set of observations including 77 Virgo galaxies matching these selection criteria. Furthermore 36 galaxies in the Coma/A1367 supercluster and 12 in A2197 and A2199, observed as fillers are presented.
The target galaxies are listed in Table 1 as follows:

- Column 1: VCC designation, from Binggeli et al. (1985) for Virgo galaxies, or CGCG (Zwicky et al. 1961–68) for Coma supercluster and A2197 and A2199 galaxies;
- Column 2: NGC/IC name;
- Column 3: UGC name (Nilson 1973);
- Columns 4 and 5: J2000 celestial coordinates, from NED;
- Columns 6 and 7: major an minor optical diameters (arcmin). For VCC galaxies the diameters are measured on the du Pont plates at the faintest detectable isophote, as listed in the VCC. For CGCG galaxies these are the major and minor optical diameters (a_{25}, b_{25}) derived as explained in Gavazzi & Boselli (1996);
- Column 8: heliocentric velocity (km s^{-1}) from the VCC or from Gavazzi et al. (1999a);
- Column 9: the membership to a cluster or supercluster, defined as in Gavazzi et al. (1999a) for Virgo and Gavazzi et al. (1999b) for the Coma/A1367 supercluster;
- Column 10: the distance (Mpc); we assume the average values for the different substructures of Virgo as given in Gavazzi et al. (1999a), 96 Mpc for galaxies in Coma, 91 Mpc for A1367, 125 Mpc for A2197 and 122 Mpc for A2199. For galaxies not belonging to the clusters, the distance is determined from the redshift assuming $H_0 = 75$ km s^{-1} Mpc^{-1};
- Column 11: projected angular distance from the cluster centre (degrees);
- Column 12: morphological type as given in the VCC or in Gavazzi & Boselli (1996);
- Column 13: photographic magnitude as given in the VCC or in the CGCG;
- Column 14: B magnitude determined and corrected for dust extinction as described in Gavazzi & Boselli (1996);
- Column 15: asymptotic H band magnitude, uncorrected for extinction, determined as described in Gavazzi et al. (2000).

3. Observations

Narrow band imaging in the Hα emission line (λ = 6562.8 Å) of 125 galaxies was obtained during 13 nights distributed in 3 runs (1999, 2000 and 2001), using the 2.1 m telescope at San Pedro Martir Observatory (SPM) (Baja California, Mexico). The (f/7.5) SPM Cassegrain focus was equipped in 1999–2000 with a thinned TK1024× 1024 pixels CCD detector with pixel size is 0.30 arcsec. In 2001 we used a Thompson 1024×1024 pixels CCD detector with pixel size is 0.36 arcsec. Each galaxy was observed through two narrow band interferometric filters centered at λ 6603 and λ 6723 Å, with a width of ∼90 Å. The λ 6603 Å was selected to cover the Hα line (ON-band filter) for galaxies at the redshift of Virgo (with $350 < V < 3000$ km s^{-1}) and to recover the red continuum (OFF-band) for higher redshift objects (in the Coma and Hercules superclusters). The λ 6723 Å filter provided us with the OFF-band frames for Virgo and the ON-band frames for higher redshift objects. The typical integration time was of 15–40 min, equal for the ON- and OFF-band, generally split into 3 shorter exposures. The observations were obtained with seeing ranging from 1.8 to 3 arcsec, but mostly in photometric conditions. The observations were flux calibrated using the standard stars Feige 34 and Hz44 from the catalogue of Massey et al. (1988), observed every 2 hours. Repeated measurements gave <0.05 mag differences, which we assume as the typical uncertainty (1σ) of the photometric results given in this work. Most frames were obtained in these conditions. Some were obtained in transparent conditions ($0.05 < \sigma < 0.10$ mag) and few were observed through thin cirrus ($\sigma > 0.10$ mag). For the latter we don't derive the flux but the Hα equivalent width only.

4. Image analysis

The reduction of the CCD frames follows a procedure similar to the one described in previous papers (e.g. Gavazzi et al. 1998), based on the IRAF STSDAS[1] reduction packages. To remove the detector response each image was

[1] IRAF is the Image Analysis and Reduction Facility made available to the astronomical community by the National Optical Astronomy Observatories, which are operated by AURA, Inc., under contract with the U.S. National Science Foundation. STSDAS is distributed by the Space Telescope Science Institute, which is operated by the Association of Universities for Research in Astronomy (AURA), Inc., under NASA contract NAS 5–26555.

Table 1. The target galaxies.

Virgo														
VCC	NGC/IC	UGC	RA($J2000$)	Dec	a	b	Vel	Clust.	Dist	θ	Type	$m_{\rm pg}$	$B^0_{\rm T}$	$H_{\rm T}$
(1)	(2)	(3)	(4)	(5)	(6)	(7)	(8)	(9)	(10)	(11)	(12)	(13)	(14)	(15)
1	-	-	120 820.02	134 100.2	0.80	0.18	2267	M	32	5.63	BCD	14.78	15.90	12.50
25	4152	7169	121 037.23	160 159.5	2.54	1.71	2169	M	32	6.09	Sc	12.46	12.47	9.84
47	4165	7201	121 211.77	131 447.8	1.41	0.76	1862	M	32	4.62	Sa	14.20	14.00	-
49	4168	7203	121 216.46	131 223.9	1.76	1.40	2307	M	32	4.60	E	12.21	12.63	8.71
58	769	7209	121 232.21	120 725.9	2.54	1.75	2207	M	32	4.48	Sb	13.17	13.36	10.51
73	4180	7219	121 302.99	70 219.0	1.88	0.68	2082	W	32	6.91	Sb	13.35	12.74	9.48
81	4186	7223	121 326.18	144 620.1	0.95	0.81	2075	N	17	4.85	Sc	15.60	15.72	12.53
97	4193	7234	121 353.65	131 022.2	1.96	0.97	2476	M	32	4.20	Sc	13.20	12.81	9.60
105	-	7239	121 408.90	74 634.3	2.48	2.06	1221	W	32	6.18	Sd	13.68	-	-
120	4197	7247	121 438.42	54 816.4	3.60	0.64	2064	W	32	7.70	Scd	13.47	12.05	10.42
131	3061	7255	121 504.41	140 144.5	2.60	0.28	2317	N	17	4.17	Sc	14.34	12.87	-
162	3074	7279	121 546.12	104 153.7	2.92	0.50	1979	N	17	4.06	Sd	14.41	15.03	11.48
199	4224	7292	121 633.63	72 743.9	2.92	1.00	2594	W	32	6.05	Sa	12.95	12.07	8.86
221	4234	7309	121 708.62	34 050.1	1.76	1.56	2031	W	32	9.35	Sc	13.43	13.47	11.23
318	776	7352	121 903.40	85 122.7	1.71	1.00	2469	W	32	4.57	Scd	14.01	14.04	12.72
358	4264	7364	121 935.66	55 047.9	1.55	1.06	2633	B	23	7.11	Sa	13.80	13.60	10.17
362	4266	7368	121 942.19	53 216.9	2.16	0.42	1617	W	32	7.37	Sa	14.51	13.13	-
393	4276	7385	122 007.47	74 128.1	2.10	2.11	2617	B	23	5.38	Sc	13.25	13.65	10.63
449	4289	7403	122 102.34	34 319.4	4.33	0.43	2541	S	17	9.00	Sbc	14.34	12.76	-
465	4294	7407	122 117.82	113 031.5	3.95	1.24	357	N	17	2.49	Sc	12.61	11.69	9.76
492	4300	7413	122 141.45	52 304.7	2.16	0.70	2310	B	23	7.36	Sa	13.76	13.09	9.68
522	4305	7432	122 203.54	124 427.8	2.60	1.29	1888	A	17	2.17	Sa	13.19	13.07	9.98
523	4306	7433	122 204.23	124 712.8	1.87	1.16	1508	A	17	2.17	dS0	13.75	-	10.68
534	4309	7435	122 212.25	70 838.9	2.00	1.00	1071	B	23	5.66	Sa	13.59	13.50	10.09
552	-	7439	122 227.02	43 400.0	1.89	1.43	1296	S	17	8.09	Sc	13.61	13.60	-
567	3225	7441	122 238.78	64 037.1	2.16	0.56	2366	B	23	6.05	Scd	14.35	13.56	-
576	4316	7447	122 242.18	91 957.1	2.48	0.50	1254	B	23	3.65	Sbc	13.70	12.86	9.61
593	3229	7448	122 252.67	64 045.1	1.15	0.28	1540	B	23	6.04	S(dS)	15.08	14.92	-
613	4324	7451	122 306.12	51 500.2	3.52	1.00	1670	S	17	7.39	Sa	12.60	11.95	8.67
667	3259	7469	122 348.48	71 111.5	1.71	0.84	1420	B	23	5.49	Sc	14.24	13.83	10.85
699	3268	7477	122 407.44	63 626.7	1.95	1.37	727	B	23	6.01	Pec	14.22	13.47	11.13
713	4356	7482	122 414.10	83 203.7	3.20	0.50	1137	B	23	4.18	Sc	14.04	12.44	9.81
739	0	-	122 440.51	31 810.9	2.00	2.00	927	S	17	9.22	Sd	14.36	-	-
768	3298	-	122 503.69	170 057.1	1.03	0.27	2434	A	17	4.83	Sc	14.91	14.32	12.51
785	4378	7497	122 517.90	45 529.2	3.06	2.48	2557	S	17	7.59	Sa	12.16	12.49	8.41
827	-	7513	122 542.71	71 255.4	3.60	0.43	992	B	23	5.33	Sc	13.76	12.49	9.85
851	3322	7518	122 554.06	73 313.5	2.16	0.50	1195	B	23	4.99	Sc	14.14	13.27	10.77
859	-	7522	122 558.18	32 537.5	2.92	0.37	1428	S	17	9.05	Sc	14.61	13.07	-
921	4412	7536	122 635.80	35 756.8	1.89	1.57	2289	S	17	8.49	Sbc	13.14	13.41	10.44
950	3356	7547	122 651.38	113 316.9	1.71	0.84	1098	A	17	1.28	Sm	14.49	15.76	-
951	3358	7550	122 654.36	114 006.0	1.43	0.94	2066	A	17	1.20	E/dS0	14.35	14.58	11.60
971	4423	7556	122 708.93	55 248.1	3.06	0.43	1120	B	23	6.57	Sd	14.28	14.16	11.21
980	3365	7563	122 711.26	155 350.1	2.48	1.00	2342	A	17	3.61	Scd	14.17	14.65	-
989	-	-	122 717.39	74 012.1	0.67	0.50	1846	S	17	4.79	Sc	15.80	-	-
1011	-	7567	122 729.18	73 838.2	1.29	0.55	874	S	17	4.82	Sdm	14.85	-	12.40
1091	-	7590	122 818.70	84 346.7	1.45	0.42	1119	B	23	3.71	Sbc	14.60	13.65	-
1118	4451	7600	122 840.50	91 532.9	1.96	0.96	865	B	23	3.18	Sc	13.31	12.92	10.07
1126	3392	7602	122 843.26	145 958.9	2.92	1.16	1687	A	17	2.66	Sc	13.30	12.45	9.39
1193	4466	7626	122 930.59	74 148.3	1.20	0.34	757	S	17	4.71	Sc	14.61	13.41	11.23
1249	-	7636	123 000.94	75 545.6	1.45	1.03	468	S	17	4.47	Im	14.75	15.80	13.37
1290	4480	7647	123 026.47	41 452.8	2.01	1.07	2438	S	17	8.14	Sb	13.09	12.85	9.78
1330	4492	7656	123 059.58	80 439.1	1.96	1.96	1777	S	17	4.30	Sa	13.17	13.15	9.42
1356	3446	-	123 122.92	112 934.3	1.10	0.43	1251	A	17	0.91	Sm/BCD	15.50	15.56	12.85
1379	4498	7669	123 139.62	165 107.5	2.85	1.53	1505	A	17	4.46	Sc	12.61	12.30	9.97
1393	797	7676	123 154.59	150 726.6	1.68	1.11	2100	A	17	2.74	Sc	14.01	13.41	10.94
1410	4502	7677	123 203.22	164 114.7	1.48	0.78	1629	A	17	4.31	Sm	14.57	14.54	11.86
1411	3466	-	123 204.83	114 902.7	0.69	0.42	911	A	17	0.65	Pec	15.72	15.53	-
1426	-	-	123 222.80	115 338.9	0.80	0.80	1110	A	17	0.63	Im	15.64	16.43	-
1429	3467	7686	123 224.01	114 714.9	1.00	0.14	7506	bg	101	0.71	Sc	15.41	-	-
1442	3474	7687	123 236.78	23 943.1	2.92	0.36	1735	S	17	9.74	Sd	14.82	14.88	-

Table 1. continued.

Virgo														
VCC	NGC/IC	UGC	RA(J2000)	Dec	a	b	Vel	Clust.	Dist	θ	Type	$m_{\rm pg}$	$B^0_{\rm T}$	$H_{\rm T}$
(1)	(2)	(3)	(4)	(5)	(6)	(7)	(8)	(9)	(10)	(11)	(12)	(13)	(14)	(15)
1491	3486	-	123 313.98	125 127.4	0.80	0.61	1903	A	17	0.75	dE	15.24	15.58	11.64
1508	4519	7709	123 330.08	83 916.6	3.60	2.60	1212	S	17	3.79	Sc	12.34	12.14	9.73
1532	800	7716	123 356.79	152 116.9	1.87	1.36	2335	A	17	3.06	Sc	14.05	13.65	10.73
1557	4533	7725	123 422.11	21 931.1	2.60	0.43	1759	S	17	10.10	Scd	14.50	13.30	11.74
1581	-	7739	123 444.93	61 807.4	1.46	1.15	2065	S	17	6.16	Sm	14.55	15.08	-
1624	4544	7756	123 536.17	30 204.9	2.48	0.50	1151	S	17	9.43	Sc	13.89	12.98	10.35
1654	3562	-	123 610.23	95 523.3	0.84	0.27	2051	A	17	2.79	Im	15.96	-	14.32
1675	-	-	123 634.65	80 317.6	1.26	0.74	1795	S	17	4.56	Pec	14.47	-	12.31
1686	3583	7784	123 643.57	131 531.7	2.79	1.71	1122	A	17	1.68	Sm	13.95	13.46	11.00
1699	3589	7790	123 702.24	65 530.9	1.55	0.82	1635	S	17	5.67	Sm	14.10	14.44	-
1757	4584	7803	123 817.79	130 635.8	1.87	1.00	1783	A	17	1.96	Sa	13.60	13.59	10.56
1758	-	7802	123 820.81	75 328.8	1.71	0.27	1788	S	17	4.87	Sc	14.99	13.66	11.72
1789	-	-	123 921.34	45 619.5	1.10	0.62	1619	S	17	7.74	Im	15.07	15.91	12.60
1791	3617	7822	123 924.45	75 752.5	1.29	0.64	2079	S	17	4.90	Sm/BCD	14.67	14.66	-
1918	-	-	124 218.10	54 421.7	1.03	0.35	980	S	17	7.23	Im	15.80	-	-
1923	4630	7871	124 231.37	35 736.9	2.31	1.60	742	S	17	8.91	Sbc	13.14	12.88	9.91
2023	3742	7932	124 531.55	131 951.3	2.01	1.00	958	E	17	3.70	Sc	13.86	13.54	11.37

bias subtracted and divided by the median of several flat field exposures obtained on empty regions of the twilight sky. When three images in the same filter were available, a median combination of the realigned images allows removal of cosmic rays. For galaxies observed in single exposures these were removed manually by direct inspection of the frames. Subtraction of contaminating objects, such as nearby stars and galaxies, was done by direct inspection of the frames. The sky background was determined in each frame in concentric object-free annuli around the object and then subtracted from the flat-fielded image. The typical uncertainty on the mean background is estimated 10% of the rms in the individual pixels. This represents the dominant source of error in low S/N regions.

4.1. Hα + [NII] parameters

The flux from the [NII] emission lines (λ 6548–6584 Å) bracketing Hα are included in the ON-band observations. Herafter we will use the semplified notation "Hα" to refer to "Hα + [NII]". Both the flux and the EW of the Hα line can be recovered from narrow band observations by subtracting the continuum contribution, determined in the OFF-band frame, from the ON-band frame (continuum+line), provided that the two filters have identical profiles. This is generally not true, however the ratio n of their integrated profiles can be determined assuming that field stars (with null Hα in emission) have identical fluxes in the ON- and OFF-band frames.

The total counts in the two frames have been obtained by integrating the pixel counts over the area covered by each galaxy, as derived from their optical axes a and b. If $C_{\rm ON}$ and $C_{\rm OFF}$ represent the integrated pixel counts in the ON and OFF-band filter respectively,
$C_{\rm NET} = C_{\rm ON} - nC_{\rm OFF}$
then the net flux in the Hα line is given by:

$$F({\rm H}\alpha) = 10^{Z{\rm p}} \frac{C_{\rm NET}}{T R_{\rm ON}({\rm H}\alpha)} \quad (1)$$

and the equivalent width by:

$${\rm H}\alpha EW = \frac{\int R_{\rm ON}(\lambda){\rm d}\lambda}{R_{\rm ON}({\rm H}\alpha)} \frac{C_{\rm NET}}{nC_{\rm OFF}} \quad (2)$$

where T is the integration time (s), $10^{Z{\rm p}}$ is the ON-band zero point (erg cm^{-2} s^{-1}) corrected for atmosferic extinction and $R_{\rm ON}(\lambda)$ is the trasmissivity of the ON-filter at the wavelength of the redshifted Hα line.

Equation (2) shows that the Hα equivalent width does not depend on Zp, but only on the normalization constant n, thus it can be estimated also in marginal photometric conditions.

Due to an unfortunate choice of the OFF-band filter (λ6723 Å), Virgo galaxies ($350 < V < 3000$ km s^{-1}) have their [SII] emission doublet (λ6717–6731 Å) inside the transmission window of the OFF-band filter (see Fig. 1). Thus the contribution of these two lines must be subtracted to estimate the continuum. To do so we determine $R_{\rm OFF}(\lambda)$: the trasmissivity of the OFF-filter at the wavelength of the redshifted [SII] lines. The factor K, accounting for the [SII] contamination is:

$$K = 1 - \frac{F([{\rm SII}]_1)}{F({\rm H}\alpha)} \frac{R_{\rm OFF}([{\rm SII}]_1)}{R_{\rm ON}({\rm H}\alpha)} - \frac{F([{\rm SII}]_2)}{F({\rm H}\alpha)} \frac{R_{\rm OFF}([{\rm SII}]_2)}{R_{\rm ON}({\rm H}\alpha)} \quad (3)$$

Table 1. continued.

CGCG (1)	NGC/IC (2)	UGC (3)	RA(J2000) (4)	Dec (5)	a (6)	b (7)	Vel (8)	Clust. (9)	Dist (10)	θ (11)	Type (12)	$m_{\rm pg}$ (13)	$B^0_{\rm T}$ (14)	$H_{\rm T}$ (15)
Coma/A1367 supercluster														
97005	-	-	113 247.12	200 214.8	0.90	0.48	6129	Isol	81	2.74	Sc	15.50	15.00	12.41
97023	-	-	113 651.53	200 017.2	0.72	0.70	6320	Group	84	1.78	S0	15.30	15.44	11.80
97026	-	6583	113 654.20	195 816.6	0.79	0.48	6202	Group	84	1.77	Pec	13.90	14.09	11.49
97027	-	-	113 654.35	195 949.1	0.94	0.63	6630	Group	84	1.77	Sc	14.60	14.60	11.60
97063	-	-	114 215.51	200 254.0	0.57	0.34	6102	A1367	91	0.55	Pec	15.60	15.84	13.20
97064	-	-	114 214.52	200 549.5	0.65	0.44	5976	A1367	91	0.57	S(dS)	15.60	15.78	12.50
97068	-	-	114 224.47	200 706.3	1.23	0.76	5974	A1367	91	0.55	Sbc	14.60	14.38	11.27
97076	-	6680	114 302.10	193 859.9	1.20	0.54	7060	A1367	91	0.36	Sb	15.50	-	11.39
97079	-	-	114 313.35	200 016.4	0.75	0.45	6996	A1367	91	0.33	Pec	15.70	15.41	13.15
97130	3864	-	114 515.66	192 331.3	0.68	0.53	6697	A1367	91	0.48	Sa	15.50	15.50	11.86
97134	3867	6731	114 529.59	192 400.0	1.31	0.44	7466	A1367	91	0.50	S0	14.60	14.28	9.57
97135	3868	-	114 529.93	192 640.7	0.73	0.49	6385	A1367	91	0.46	S0	14.80	15.14	10.86
101033	-	8407	132 250.14	194 125.9	1.20	0.20	6729	Isol	89	9.80	Sc	15.70	-	12.29
101049	-	8448	132 639.89	195 640.6	1.15	0.91	7148	Isol	95	10.09	Sbc	14.90	14.24	11.49
127026	-	6645	114 056.23	254 650.9	1.12	0.87	6871	Isol	91	6.01	Sbc	14.80	14.76	11.30
127061	3911	6795	114 922.24	245 616.2	1.20	1.02	5954	Isol	79	5.24	Sc	15.40	15.07	12.99
130005	-	-	130 410.75	221 723.1	0.76	0.50	7058	Isol	93	5.77	Sbc	15.50	14.95	12.24
130025	-	8343	131 641.82	215 846.3	1.30	1.03	7001	Isol	93	7.10	Sa	15.50	14.85	11.18
130026	867	8353	131 719.62	203 816.5	1.26	1.11	6870	Group	91	8.33	Sc	15.50	14.52	11.43
130028	868	-	131 728.43	203 639.9	0.81	0.71	6714	Group	89	8.38	E	15.40	14.59	11.07
130029	870	-	131 730.81	203 555.0	0.81	0.57	6743	Group	89	8.40	Sc	15.40	14.47	11.44
131008	-	8457	132 730.58	205 247.9	1.20	0.20	5972	Isol	79	9.48	Sbc	15.60	14.29	11.16
157062	-	6932	115 728.50	310 503.8	1.10	0.26	6882	Isol	91	11.64	Pec	15.50	14.48	14.53
159037	4585	-	123 813.31	285 614.1	0.86	0.58	7291	Isol	97	4.86	Sab	14.60	14.48	11.50
159071	-	-	124 543.41	292 558.5	1.08	0.82	6924	Isol	92	3.43	Sc	15.50	14.90	12.78
159072N	4676	7938	124 610.19	304 354.6	2.20	0.40	6631	Pair	88	4.07	Pec	14.80	12.93	10.74
159072S	-	7939	124 611.38	304 324.9	1.70	0.60	6590	Pair	87	4.05	Pec	14.80	13.53	10.85
160001	-	-	125 351.45	285 843.0	0.80	0.41	7945	A1656	96	1.65	Sb	15.60	15.26	12.49
160009	-	-	125 432.95	282 234.7	0.80	0.47	7132	A1656	96	1.25	S(dS)	15.50	15.07	11.44
160108	-	-	130 212.74	281 252.9	0.46	0.43	8323	A1656	96	0.56	Pec	15.50	15.73	12.90
160110	-	-	130 221.41	281 349.2	0.59	0.28	5733	A1656	96	0.59	S0	15.20	15.50	11.73
160111	-	-	130 221.50	281 521.2	0.60	0.30	7149	A1656	96	0.61	E	15.70	15.91	12.06
160141	-	-	130 713.15	280 248.0	0.50	0.45	7292	A1656	96	1.61	Pec	15.50	15.72	12.51
161040	-	-	132 324.64	263 240.7	0.73	0.40	7260	Isol	96	5.41	Sc	15.60	15.50	12.85
161052	-	-	132 651.44	263 528.4	0.29	0.29	7072	Isol	94	6.15	Pec	15.10	15.40	12.42
161054	4256	-	132 703.07	305 834.3	0.80	0.46	6767	Isol	90	6.62	Sa	15.50	15.31	12.84
A2197/A2199														
224003	-	10354	162 121.97	404 837.5	1.00	0.84	8946	A2197	122	1.57	Sc	15.60	15.11	-
224012	-	-	162 337.85	391 211.4	0.60	0.55	8370	A2199	125	1.04	S(dS)	15.70	15.68	-
224017	6145	-	162 502.24	405 648.1	0.95	0.40	8779	A2197	122	0.89	Sc	15.10	14.28	11.34
224026	-	-	162 652.77	411 513.5	1.00	0.90	8580	A2197	122	0.69	Sc	15.20	14.69	-
224035	-	10404	162 811.60	394 918.7	1.18	0.86	8312	A2199	125	0.28	Sa	15.50	14.26	-
224039	6166	10409	162 838.55	393 307.5	1.95	1.40	9284	A2199	125	0.01	E	13.90	13.40	9.82
224040	-	-	162 844.28	392 826.9	0.80	0.80	9167	A2199	125	0.08	Sab	15.40	-	11.44
224045	-	-	162 853.01	393 337.4	0.55	0.50	8794	A2199	125	0.02	S(dS)	15.60	-	-
224057	-	10429	163 033.37	394 949.2	1.10	0.90	7392	A2199	125	0.45	Sab	15.30	-	-
224059	-	10430	163 026.78	412 900.9	1.10	1.00	8967	A2197	122	0.68	Sb	15.40	14.71	11.24
224066	-	10436	163 103.74	410 920.3	1.31	1.28	9064	A2197	122	0.42	Sc	14.80	14.57	11.14
224070	6184	-	163 134.51	403 356.4	1.23	0.80	8331	A2197	122	0.43	Sb	15.10	14.33	-

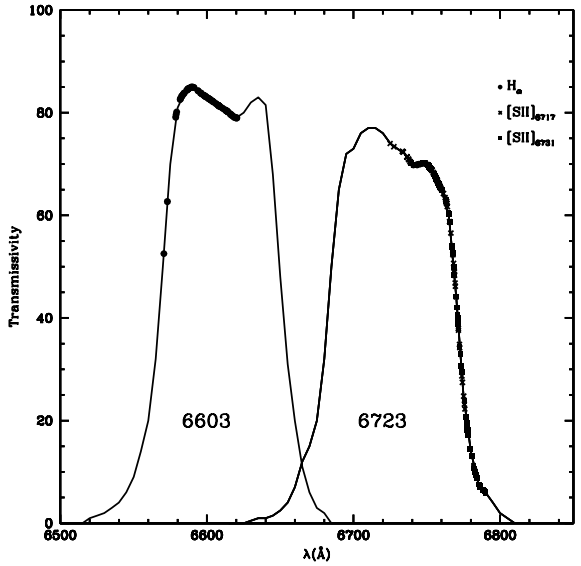

Fig. 1. The profiles of the 6603 and 6723 Å filters. Filled circles mark the transmission at Hα of Virgo galaxies. Filled squares and crosses mark the transmission at [SII] of Virgo galaxies.

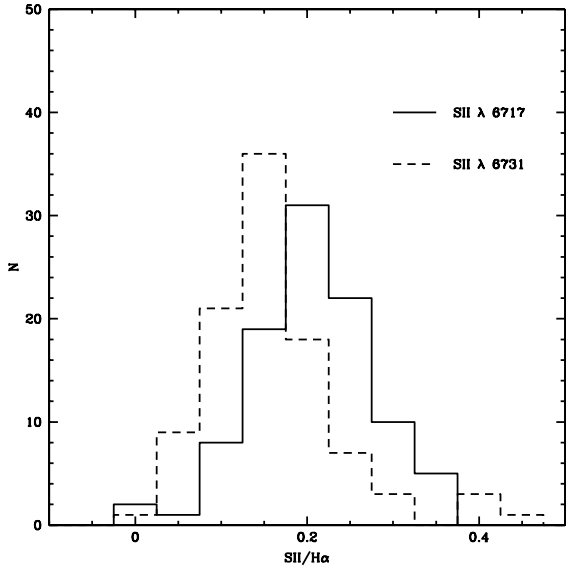

Fig. 2. Histograms of the $F([\mathrm{SII}])/F(\mathrm{H}\alpha)$ ratios determined from spectroscopy.

where $[\mathrm{SII}]_1$ is the line at λ6717 Å and $[\mathrm{SII}]_2$ is the one at λ6731 Å.

For 24 galaxies the ratios $F([\mathrm{SII}])/F(\mathrm{H}\alpha)$ of the two [SII] lines are known from spectroscopy (Gavazzi et al. 2002b) (see Fig. 2). When this measurement is not available their average values: $< F([\mathrm{SII}]_{6717})/F(\mathrm{H}\alpha) > = 0.21 \pm 0.09$ and $< F([\mathrm{SII}]_{6731})/F(\mathrm{H}\alpha) > = 0.17 \pm 0.15$ are assumed.

Accounting for the [SII] contamination, Eq. (1) becomes:

$$F(\mathrm{H}\alpha) = 10^{Z_\mathrm{P}} \frac{C_\mathrm{NET}}{T R_\mathrm{ON}(\mathrm{H}\alpha) K} \tag{4}$$

and Eq. (2) becomes:

$$\mathrm{H}\alpha EW = \frac{\int R_\mathrm{ON}(\lambda)\mathrm{d}\lambda}{R_\mathrm{ON}(\mathrm{H}\alpha)} \frac{C_\mathrm{NET}}{C_\mathrm{ON}(K-1) + nC_\mathrm{OFF}}. \tag{5}$$

For extended sources the dominant source of error is associated with the variations of the background on scales similar to the source, which depends on the quality of the flat-fielding. We measured the background in several regions comparable with the size of the galaxies and determined that its fluctuation (per pixel) is 10% of the purely statistical rms on the individual pixels. The total uncertainty on the ON and OFF counts is thus proportional to the area A (in pixels) covered by each galaxy, estimated from the optical major and minor axes, a and b.

$\sigma_\mathrm{ON} = 0.1\ \mathrm{rms}_\mathrm{ON}\ A$

$\sigma_\mathrm{OFF} = 0.1\ \mathrm{rms}_\mathrm{OFF}\ A$

which add up to:

$\sigma_\mathrm{NET} = \sqrt{(\sigma_\mathrm{ON})^2 + (\sigma_\mathrm{OFF})^2 + (0.1\ C_\mathrm{NET})^2}$.

The term $(0.1\ C_\mathrm{NET})^2$ accounts for the uncertainty on the photometric calibration.

The errors on the Hα flux and equivalent width are finally:

$$\sigma_F = \frac{F(\mathrm{H}\alpha)}{C_\mathrm{NET}} \sigma_\mathrm{NET} \tag{6}$$

$$\sigma_{EW} = \frac{\int R_\mathrm{ON}(\lambda)\mathrm{d}\lambda}{R_\mathrm{ON}(\mathrm{H}\alpha)(C_\mathrm{ON}(K-1) + nC_\mathrm{OFF})^2} \sqrt{\Sigma} \tag{7}$$

where:
$\Sigma = (2-K)^2 (nC_\mathrm{OFF})^2 \sigma^2_\mathrm{ON} + K^2 C^2_\mathrm{ON} \sigma^2_\mathrm{OFF}$.

5. Results

The results of the present observations are listed in Table 2 as follows:

- Column 1: galaxy designation;
- Column 2: date of the observation;
- Column 3: number of combined exposures;
- Column 4: integration times in minutes of the individual exposures;
- Column 5: transmissivity of the ON-band filter at the redshifted Hα line;
- Column 6: Normalization factor of the OFF-band frame;
- Column 7: a flag indicating whether the frame was taken under photometric (P) or Transparent (T) conditions or through light cyrrus (C);
- Column 8: correction factor for the contamination by the two lines of [SII] (see Eq. (3));
- Column 9: Hα+[NII] equivalent width and error, in Å;
- Column 10: Logarithm of the Hα+[NII] flux, in erg cm^{-2} s^{-1}. This quantity is given if the flag in Col. 7 is P or T;
- Column 11 and 12: Hα+[NII] equivalent width and flux from the literature, with references.

Table 2. The results of the observations.

Virgo											
VCC	Date	N	T	R(Hα)	n	Phot	K	EW(Hα) Å	F(Hα) erg cm^{-2} s^{-1}	EW(Hα)(ref) Å	F(Hα)(ref) erg cm^{-2} s^{-1}
(1)	(2)	(3)	(4)	(5)	(6)	(7)	(8)	(9)	(10)	(11)	(12)
1	18-4-1999	3	7	0.81	1.10	P	0.76	11.6 ± 0.9	−13.51 ± 0.05	14(11)	
25	19-4-2001	3	5	0.81	1.10	P	0.82	58.0 ± 2.5	−11.70 ± 0.04	46(11), 33(1)	−11.85(1)
47	18-4-1999	3	5	0.82	1.10	P	0.77	16.4 ± 5.6	−13.04 ± 0.11	11(11)	
49	18-4-1999	3	5	0.80	1.15	P	0.85	0.1 ± 1.6	–	0(11)	
58	21-4-1999	3	5	0.81	1.10	P	0.83	14.8 ± 6.2	−12.51 ± 0.15	18(11)	
73	20-4-2001	3	5	0.81	1.18	P	0.81	11.2 ± 0.6	−12.39 ± 0.05		
81	20-4-1999	4	5	0.81	1.10	P	0.81	21.0 ± 17.8	−13.26 ± 0.27		
97	21-4-1999	3	5	0.79	1.10	P	0.94	13.9 ± 1.2	−12.33 ± 0.05	15(11)	
105	01-4-2000	4	10	0.85	1.00	P	0.71	13.6 ± 9.4	−12.89 ± 0.20		
120	19-4-1999	4	10	0.81	1.10	P	0.80	54.0 ± 2.0	−11.92 ± 0.04		
131	31-3-2000	3	7	0.80	1.00	P	0.82	22.6 ± 1.6	−12.68 ± 0.05	24(11)	
162	02-4-2000	3	10	0.82	1.00	P	0.78	30.4 ± 5.2	−12.88 ± 0.07	36(11)	
199	31-3-2000	3	10	0.79	1.00	P	0.92	10.4 ± 0.6	−12.24 ± 0.05		
221	20-4-1999	3	5	0.82	1.10	P	0.80	53.3 ± 4.9	−12.07 ± 0.05		
318	18-4-1999	3	5	0.80	1.10	P	0.85	50.6 ± 9.4	−12.51 ± 0.07	31(11)	
358	20-4-2001	3	5	0.79	1.11	P	0.93	−0.3 ± 0.7	–		
362	22-4-2001	1	5	0.83	1.11	P	0.71	−3.5 ± 1.4	–		
393	20-4-2001	3	5	0.76	1.14	P	0.93	25.3 ± 3.3	−12.34 ± 0.06	21(11)	
449	01-4-2000	3	10	0.79	1.00	P	0.91	14.5 ± 1.7	−12.76 ± 0.06		
465	19-4-2001	1	15	0.53	1.15	T	0.52	56.8 ± 3.4	−11.63 ± 0.04	64(1)	−11.65(1)
492	20-4-2001	3	5	0.80	1.29	C	0.85	6.2 ± 0.8	–		
522	20-4-1999	3	5	0.82	1.10	P	0.78	−0.0 ± 8.2	–		
523	20-4-1999	3	5	0.84	1.10	P	0.72	3.1 ± 3.7	−13.18 ± 0.36		
534	20-4-2001	3	5	0.84	1.08	T	0.71	0.1 ± 2.1	–	0(11)	
552	19-4-1999	4	5	0.85	1.10	P	0.72	48.0 ± 7.5	−12.19 ± 0.06		
567	23-4-2001	3	5	0.80	1.16	P	0.87	21.6 ± 2.3	−12.73 ± 0.06		
576	02-4-2000	3	10	0.85	1.00	P	0.72	13.8 ± 0.9	−12.49 ± 0.05		
593	23-4-2001	3	5	0.84	1.16	P	0.72	5.7 ± 1.8	−13.66 ± 0.10		
613	01-4-2000	3	7	0.83	1.00	P	0.82	5.7 ± 0.9	−12.40 ± 0.07		
667	23-4-2001	3	5	0.84	1.15	P	0.72	8.7 ± 2.6	−12.97 ± 0.09		
699	23-4-2001	3	5	0.79	1.11	P	0.68	41.6 ± 7.0	−12.27 ± 0.06		
713	31-3-2000	3	10	0.85	1.00	P	0.71	8.0 ± 1.2	−12.72 ± 0.06	8(11)	
739	23-4-2001	3	7	0.83	1.11	P	0.70	35.7 ± 14.0	−12.56 ± 0.10		
768	24-4-2001	2	5	0.80	1.11	P	0.89	42.5 ± 1.5	−12.83 ± 0.04		
785	01-4-2000	3	5	0.79	1.00	P	0.92	8.4 ± 2.1	−12.19 ± 0.10		
827	19-4-1999	4	10	0.84	1.10	P	0.72	25.8 ± 1.4	−12.25 ± 0.05	53(11)	
851	23-4-2001	3	5	0.85	1.16	P	0.61	20.1 ± 2.7	−12.55 ± 0.05	26(11)	
859	02-4-2000	3	10	0.84	1.00	P	0.72	12.7 ± 1.5	−12.82 ± 0.06		
921	19-4-1999	4	5	0.80	1.10	P	0.85	37.6 ± 3.1	−12.03 ± 0.05		
950	21-4-2001	3	10	0.85	1.17	P	0.71	23.3 ± 10.8	−13.45 ± 0.13		
951	19-4-1999	2	5	0.81	1.10	C	0.80	−0.7 ± 17.5	–		
971	01-4-2000	3	10	0.85	1.00	P	0.71	28.5 ± 2.3	−12.52 ± 0.05		
980	31-3-2000	3	10	0.80	1.00	P	0.86	40.2 ± 6.3	−12.65 ± 0.06		
989	24-4-2001	3	7	0.82	1.11	P	0.77	2.8 ± 7.3	−14.63 ± 0.82		
1011	24-4-2001	3	7	0.83	1.11	P	0.70	13.1 ± 3.5	−13.27 ± 0.08		
1091	24-4-2001	3	5	0.85	1.15	P	0.71	58.6 ± 2.1	−12.33 ± 0.04		
1118	20-4-2001	3	5	0.83	1.15	C	0.70	17.3 ± 2.0	–		
1126	19-4-1999	4	5	0.83	1.10	P	0.74	10.7 ± 4.5	−12.55 ± 0.13		
1193	23-4-2001	3	5	0.80	1.11	P	0.57	30.5 ± 2.2	−12.58 ± 0.05	30(11)	
1249	23-4-2001	4	5	0.63	1.08	P	0.60	192.3 ± 58††	−14.07 ± 0.06††		
1290	31-3-2000	3	10	0.80	1.00	P	0.89	29.7 ± 1.0	−12.09 ± 0.04		

Table 2. continued.

Virgo											
VCC	Date	N	T	R(Hα)	n	Phot	K	EW(Hα) Å	F(Hα) erg cm^{-2} s^{-1}	EW(Hα)(ref) Å	F(Hα)(ref) erg cm^{-2} s^{-1}
(1)	(2)	(3)	(4)	(5)	(6)	(7)	(8)	(9)	(10)	(11)	(12)
1330	20-4-2001	3	5	0.83	1.18	P	0.76	3.7 ± 1.4	−12.68 ± 0.13	6(11)	
1356	20-4-1999	3	5	0.85	1.10	P	0.76	43.0 ± 8.1	−13.05 ± 0.07	50(11)	
1379	24-4-2001	3	5	0.84	1.05	P	0.70	36.4 ± 3.0	−11.92 ± 0.05	34(11),	−12.06(9)
1393	21-4-2001	3	5	0.81	1.16	T	0.81	37.7 ± 2.5	−12.30 ± 0.05		
1410	18-4-1999	3	5	0.83	1.10	P	0.65	34.9 ± 9.3	−12.71 ± 0.07	28(11)	
1411	21-4-2001	3	10	0.83	1.02	P	0.70	2.1 ± 2.4	−14.37 ± 0.29		
1426	23-4-2001	3	5	0.85	1.08	P	0.71	5.9 ± 7.4	−13.93 ± 0.35		
1429	21-4-2001	3	10	0.73	1.02	P	1.00	45.3 ± 0.4	−13.04 ± 0.04		
1442	02-4-2000	3	10	0.83	1.00	P	0.75	18.2 ± 2.9	−12.97 ± 0.06		
1491	18-4-1999	3	4	0.82	1.10	P	0.78	−0.5 ± 6.4	−	0(11)	
1508	24-4-2001	3	5	0.85	1.12	P	0.71	39.7 ± 5.5	−11.78 ± 0.06		−11.75(9)
1532	20-4-2001	3	5	0.80	1.17	P	0.86	17.3 ± 2.5	−12.55 ± 0.07		
1557	02-4-2000	3	10	0.83	1.00	P	0.76	23.5 ± 2.3	−12.74 ± 0.05		
1581	23-4-2001	3	10	0.81	1.18	P	0.80	5.8 ± 3.5	−13.46 ± 0.20		−13.24(4)
1624	02-4-2000	3	7	0.85	1.00	P	0.71	11.5 ± 2.3	−12.82 ± 0.07		
1654	24-4-2001	3	7	0.81	1.18	P	0.80	19.4 ± 2.5	−13.57 ± 0.06		
1675	20-4-1999	3	5	0.83	1.10	P	0.68	4.2 ± 10.3	−13.85 ± 0.68	13(11)	
1686	17-4-1999	4	7	0.85	1.10	P	0.68	43.5 ± 12.2	−12.17 ± 0.08	56(11)	
1699	21-4-2001	3	7	0.83	1.12	P	0.73	24.0 ± 4.2	−12.85 ± 0.06		−12.33(4)
1757	01-4-2000	3	5	0.83	1.00	P	0.70	7.5 ± 4.8	−12.98 ± 0.19	8(11)	
1758	18-4-1999	3	5	0.83	1.10	P	0.76	17.0 ± 3.3	−13.07 ± 0.07		
1789	21-4-2001	3	7	0.83	1.12	P	0.73	16.4 ± 3.6	−13.25 ± 0.08		
1791	24-4-2001	3	5	0.81	1.13	P	0.84	71.6 ± 3.5	−12.42 ± 0.05	80(11)	
1918	21-4-2001	3	7	0.84	1.13	P	0.71	14.6 ± 8.1	−13.90 ± 0.15		
1923	20-4-2001	3	5	0.80	1.15	P	0.68	36.0 ± 3.6	−11.93 ± 0.05		
2023	19-4-2001	3	5	0.84	1.10	P	0.70	27.5 ± 5.4	−12.56 ± 0.07		

Galaxies with substantial Hα structure are shown in Fig. 4. The OFF-frames are displayed with contours superposed to the NET-frames, given in grey-scale.

5.1. Comparison with the literature

Few galaxies measured in this work have independent imaging measurements in the literature (see Table 2). However 24 objects were spectroscopically observed (Gavazzi et al. 2002b) in the "drift-scan" mode, with the slit sliding over most of the galaxy surface. Spectra taken in this way are representative of the mean galaxy, unlike most long slit observations which are dominated by the nuclear light. Hα + [NII] equivalent widths from spectroscopy are thus directly comparable with our imaging data, as illustrated in Fig. 3, showing a satisfactory agreement. The average differences between our flux and equivalent width estimates and those in the literature are: Hα + [NII]$EW_{\rm TW}$ − Hα + [NII]$EW_{\rm L}$ = −5.2 ± 2.9 (Å) and $-\log F({\rm H}\alpha+[{\rm NII}])_{\rm TW}+\log F({\rm H}\alpha+[{\rm NII}])_{\rm L} = -0.12\pm 0.1$ (erg cm^{-2} s^{-1})

6. Summary

Hα+[NII] surface photometry of 125 galaxies obtained with the 2.1 m SPM telescope is presented. We derive Hα+[NII] fluxes and equivalent widths and we show the images of the detected galaxies. These observations are aimed at completing the Hα survey of galaxies in the Virgo cluster and in other clusters, as well as of relatively isolated objects in the Coma supercluster, thus spanning a large range of morphological type, luminosity and environmental conditions. Combining the results of the present work with those given in Papers II and III of this series and with the ones available from the literature 235/312 (75%) late-type Virgo cluster members have Hα measurements, as well as 177/256 (69%) late-type members to the Coma supercluster. The analysis of the current ($<10^7$ yr)

Table 2. continued.

CGCG	Date	N	T	R(Ha)	n	Phot	K	EW(Hα) Å	F(Hα) erg cm^{-2} s^{-1}	EW(Hα)(ref) Å	F(Hα)(ref) erg cm^{-2} s^{-1}
(1)	(2)	(3)	(4)	(5)	(6)	(7)	(8)	(9)	(10)	(11)	(12)
Coma/A1367 supercluster.											
97005	18-4-1999	3	7	0.73	1.10	P	1.00	39.0 ± 0.1	−12.86 ± 0.04		
97023	21-4-2001	3	5	0.73	1.10	P	1.00	1.0 ± 0.9	−14.30 ± 0.38		
97026	21-4-2001	3	5	0.73	1.11	P	1.00	83.1 ± 0.8	−12.23 ± 0.04	88(2)	− 12.26(2)
97027	21-4-2001	3	5	0.77	1.11	P	1.00	22.0 ± 0.9	−12.89 ± 0.05		
97063	22-4-2001	3	5	0.72	1.11	P	1.00	22.1 ± 1.6	−13.47 ± 0.05	12(10)	− 13.69(10)
97064	22-4-2001	3	5	0.71	1.13	P	1.00	0.5 ± 1.1	−14.82 ± 0.95		
97068	22-4-2001	3	5	0.71	1.13	P	1.00	40.6 ± 1.6	−12.50 ± 0.05	41(7)	− 12.6(7)
97076	31-3-2000	3	10	0.77	1.13	P	1.00	1.0 ± 0.7	−14.28 ± 0.31		
97079	01-4-2000	3	7	0.77	1.00	P	1.00	128.9 ± 3.0	−12.66 ± 0.04	137(8)	− 12.66(8)
97130	21-4-1999	3	5	0.77	1.00	P	1.00	− 2.0 ± 0.1	–		
97134	21-4-1999	3	5	0.74	1.10	P	1.00	− 2.1 ± 0.0	–		
97135	21-4-1999	3	5	0.74	1.10	P	1.00	− 1.2 ± 0.0	–		
101033	01-4-2000	3	7	0.77	1.10	P	1.00	16.2 ± 1.2	−13.54 ± 0.05		
101049	17-4-1999	4	5	0.76	1.00	P	1.00	9.9 ± 0.2	−13.08 ± 0.04		
127026	19-4-1999	4	5	0.77	1.10	P	1.00	14.7 ± 0.2	−12.90 ± 0.04		
127061	19-4-1999	4	5	0.70	1.10	P	1.00	29.4 ± 0.5	−12.97 ± 0.04		
130005	21-4-1999	3	5	0.77	1.10	P	1.00	40.5 ± 0.2	−12.89 ± 0.04		
130025	01-4-2000	3	10	0.77	1.10	P	1.00	0.5 ± 1.1	−14.46 ± 0.92		
130026	20-4-2001	2	5	0.77	1.00	P	1.00	17.6 ± 5.0	−12.87 ± 0.12		
130028	20-4-2001	2	5	0.77	1.14	P	1.00	2.2 ± 1.7	−13.73 ± 0.33		
130029	20-4-2001	2	5	0.77	1.14	P	1.00	54.4 ± 2.9	−12.51 ± 0.05		
131008	31-3-2000	3	10	0.71	1.14	P	1.00	27.0 ± 0.3	−12.87 ± 0.04		
157062	21-4-1999	3	5	0.77	1.00	P	1.00	77.0 ± 0.3	−12.92 ± 0.04		
159037	24-4-2001	2	5	0.75	1.28	C	1.00	44.4 ± 1.3			
159071	20-4-1999	2	5	0.77	1.10	P	1.00	32.2 ± 0.3	−13.04 ± 0.04		
159072N	19-4-2001	3	5	0.77	1.09	P	1.00	6.1 ± 0.8	−13.11 ± 0.07	18(3)†	
159072S	19-4-2001	3	5	0.77	1.09	P	1.00	11.8 ± 1.0	−12.82 ± 0.06	12(3)†	
160001	21-4-2001	3	5	0.71	1.09	T	1.00	14.6 ± 1.4	−13.37 ± 0.06		
160009	21-4-1999	3	5	0.76	1.10	P	1.00	5.6 ± 0.1	−13.51 ± 0.04		
160108	18-4-1999	3	5	0.70	1.10	P	1.00	37.4 ± 0.2	−13.05 ± 0.04		
160110	18-4-1999	3	5	0.60	1.10	P	1.00	− 1.8 ± 0.1	–		
160111	18-4-1999	3	5	0.76	1.10	P	1.00	1.2 ± 0.1	−14.39 ± 0.05		
160141	18-4-1999	3	5	0.75	1.10	P	1.00	30.2 ± 0.2	−13.13 ± 0.04		
161040	22-4-2001	3	5	0.75	1.16	P	1.00	20.5 ± 1.6	−13.38 ± 0.05		
161052	19-4-2001	3	5	0.77	1.13	P	1.00	44.2 ± 0.3	−12.72 ± 0.04	48(6)	− 12.67(6)
161054	24-4-2001	3	5	0.77	1.03	P	1.00	42.5 ± 1.6	−12.93 ± 0.05		
A2197/A2199											
224003	24-4-2001	3	5	0.66	1.03	P	1.00	10.1 ± 4.3	−13.39 ± 0.18		
224012	19-4-1999	4	5	0.70	1.10	P	1.00	35.8 ± 0.2	−13.08 ± 0.04		
224017	23-4-2001	3	5	0.68	1.11	P	1.00	3.8 ± 0.7	−13.51 ± 0.09		
224026	17-4-1999	3	5	0.70	1.10	P	1.00	34.3 ± 0.3	−12.71 ± 0.04		
224035	18-4-1999	3	5	0.70	1.10	P	1.00	5.3 ± 0.2	−13.35 ± 0.05		
224039	23-4-2001	3	5	0.58	1.14	P	1.00	3.5 ± 1.0	−12.86 ± 0.13		
224040	22-4-2001	3	5	0.63	1.14	P	1.00	2.0 ± 1.0	−13.82 ± 0.22		
224045	23-4-2001	3	5	0.68	1.13	P	1.00	30.8 ± 2.2	−13.27 ± 0.05		
224057	20-4-1999	3	5	0.74	1.10	P	1.00	20.7 ± 0.3	−12.97 ± 0.04		
224059	21-4-2001	3	5	0.66	0.95	C	1.00	4.2 ± 1.8	–		
224066	23-4-2001	3	5	0.64	1.10	P	1.00	6.9 ± 2.3	−13.21 ± 0.15		
224070	20-4-1999	2	5	0.70	1.10	C	1.00	12.8 ± 0.2	–		

References: (1) Kennicutt & Kent (1983); (2) Kennicutt et al. (1984); (3) Keel et al. (1985); † from nuclear spectroscopy; (4) Gallagher & Hunter (1989); (5) Romanishin (1990); (6) Gavazzi et al. (1991); (7) Moss et al. (1998); (8) Gavazzi et al. (1998); (9) Koopmann et al. (2001); (10) Iglesias et al. (2002); (11) Gavazzi et al. (2002b), from drift-scan spectroscopy.

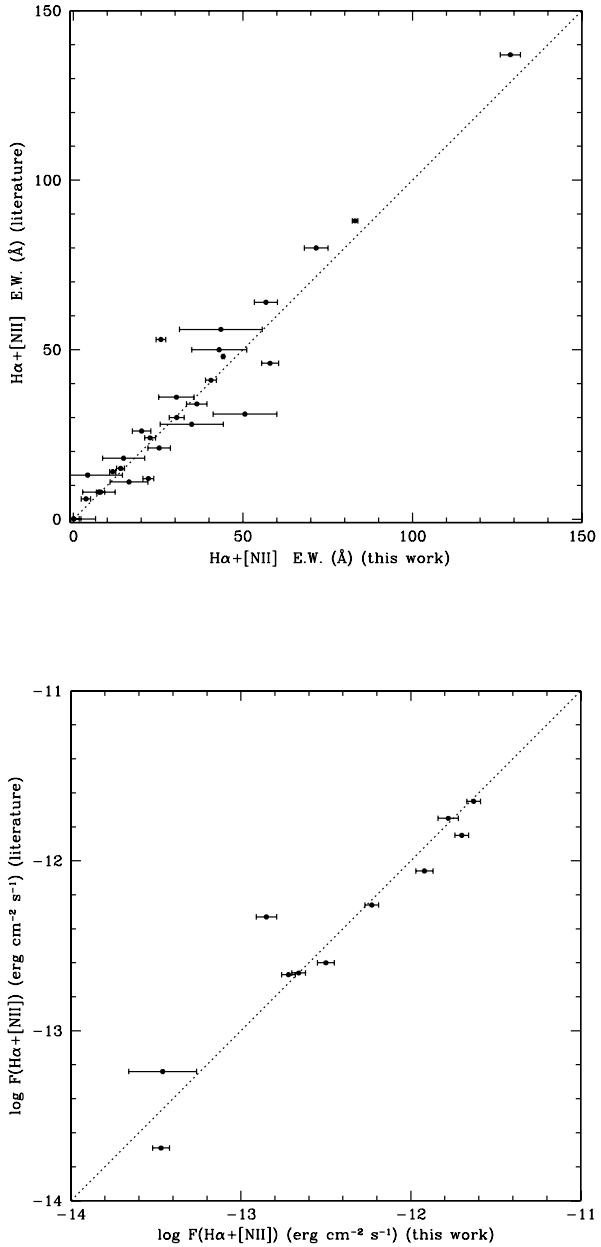

Fig. 3. comparison of the Hα+[NII]EW (top) and fluxes (bottom) determined in this work with the ones taken from the literature.

massive (>5 $M_\odot$) star formation properties of galaxies in the above regions will be carried out in the forthcoming Paper IV using the statistically significant set of observations here presented.

7. Comments on individual objects

VCC 1429 is in the background of the Virgo cluster (V = 7506 km s^{-1}). It was serendipitously observed in the field of VCC 1426 (with inverted filters).

VCC 1249 this galaxy (UGC 7636) was observed spectroscopically by Lee et al. (2000) who discovered an HII region associated with this galaxy but not spatially coincident with it, as it is found in the envelope of the giant elliptical galaxy M 49. We do not detect any Hα emission from VCC 1249 itself, but we detect the HII region (marked with an arrow in Fig. 4). The flux and EW quoted in Table 2 (††) refer to the HII region only.

Acknowledgements. We thank the night operators for their assistence during the observations and the SPM TAC for the generous time allocations. A.B. acknowledges financial support from the French GdR Galaxies. This research has made use of the NASA/IPAC Extragalactic Database (NED) which is operated by the Jet Propulsion Laboratory, California Institute of Technology, under contract with the National Aeronautics and Space Administration. L. Carrasco research is supported by CONACYT research grant G28586-E.

References

Binggeli, B., Sandage, A., & Tammann, G. 1985, AJ, 90, 1681 (VCC)
Binggeli, B., Popescu, C., & Tammann, G. 1993, A&AS, 98, 275
Boselli, A., & Gavazzi, G. 2002, A&A, 386, 124 (Paper II)
Boselli, A., Iglesias-Páramo, J., Vilchez, J., & Gavazzi, G. 2002, A&A, 386, 134 (Paper III)
Gallagher, J., & Hunter, D. 1989, AJ, 98, 806
Gavazzi, G., Boselli, A., & Kennicutt, R. 1991, AJ, 101, 1207
Gavazzi, G., & Boselli, A. 1996, Astro. Lett. & Comm., 35, 1
Gavazzi, G., Catinella, B., Carrasco, L., Boselli, A., & Contursi, A. 1998, AJ, 115, 1745
Gavazzi, G., et al. 2002a, in preparation (Paper IV)
Gavazzi, G., Boselli, A., Scodeggio, M., Pierini, D., & Belsole, E. 1999a, MNRAS, 304, 595
Gavazzi, G., Carrasco, L., & Galli, R. 1999b, A&AS, 136, 227
Gavazzi, G., Franzetti, P., Scodeggio, M., Boselli, A., & Pierini, D. 2000, A&A, 361, 863
Gavazzi, G., et al. 2002b, in preparation (Spectra)
Giovanelli, R., & Haynes, M. 1985, ApJ, 292, 404
Iglesias, J., Boselli, A., Cortese, L., Vilchez, J., & Gavazzi, G. 2002, A&A, submitted
Keel, W., Kennicutt, R., Hummel, E., & van der Hulst, J. 1985, AJ, 90, 708
Kennicutt, R. 1983, AJ, 88, 483
Kennicutt, R. 1998, ARA&A, 36, 189
Kennicutt, R., Bothun, G., & Schommer, R. 1984, AJ, 89, 1279
Kennicutt, R., & Kent, S. 1983, AJ, 88, 1094
Koopmann, R., Kenney, J., & Joung, J. 2001, ApJS, 135, 125
Lee, H., Richer, M., & McCall, M. 2000, ApJ, 530, L17
Massey, P., Strobel, K., Barnes, J., & Anderson, E. 1988, ApJ, 328, 315
Moss, C., Whittle, M., & Pesce, J. 1998, MNRAS, 300, 205
Nilson, P. 1973, Uppsala General Catalogue of Galaxies, Uppsala Obs. Ann., vol. 6, (UGC)
Roberts, M., & Haynes, M. 1984, ARA&A, 32, 115
Romanishin, W. 1990, AJ, 100, 373
Schmidt, M. 1959, ApJ, 129, 243
Young, J., Allen, L., Kenney, J., Lesser, A., & Brooks, R. 1996, AJ, 112, 1903
Zwicky, F., Herzog, E., Karpowicz, M., Kowal, C., & Wild, P. 1961–1968, Catalogue of Galaxies and of Cluster of Galaxies (Pasadena, California Institute of Technology; CGCG)